Proceedings of the 2012 IFAC Workshop on Automatic Control in Offshore Oil and Gas Production, Norwegian University of Science and Technology, Trondheim, Norway, May 31 - June 1, 2012

A Simplified Model for Multi-Fluid Dual Gradient Drilling Operations

Øyvind Nistad Stamnes * **Erlend Mjaavatten** * **Kristin Falk** *

* *Ocean Riser Systems, Lilleakerveien 2B, 0283 Oslo, Norway (e-mail: oyvind.stamnes@oceanriser.com).*

Abstract: Dual gradient drilling (DGD) is a method for drilling deep water offshore wells safely, efficiently, and to a reduced cost. The dual gradient effect is enforced by using a heavy fluid fitting the drilling window, and a subsea pump to lift the returns up to the rig. Automatic control of this pump is fundamental to ensure a safe and efficient dual gradient drilling operation. In this paper we extend existing work on modelling for DGD in two ways. Firstly, we present a simplified model for operational scenarios where there are multiple fluids in the well, e.g. when changing drilling fluids. Secondly, we make the model more realistic by including a model of the centrifugal subsea pump. The resulting model is then used to simulate a scenario with changing of drilling fluid, and where a PI controller is used to maintain a constant downhole pressure. The simulation confirms that the model is reasonable, and that the PI controller is able to maintain a near constant downhole pressure throughout the operation.

Keywords: Modelling, drilling, pressure control, PI control

1. INTRODUCTION

In this paper we present a simplified hydraulic model for multi-fluid dual gradient drilling; we focus specifically on systems with a partially filled riser as presented by Fossli and Sangesland (2006). The model can also be applied to general DGD system e.g. with water and mud (Schumacher et al. (2002)) and through small modifications extend existing work on modelling of managed pressure drilling systems (Kaasa et al. (2012)).

A partially filled riser allows for the use of heavier mud weights than conventional drilling. The results are improved margins, potential for improved casing program, improved cementing operations and improved well control and integrity. Several drilling operations require simultaneous use of more than one drilling fluid in the well, e.g. cement, spacer and mud during cementing operations. The simplified model presented here can be used for control design, estimation and simulation for these operations. A schematic of a well being drilled with a partially evacuated riser is shown in Fig. 1. The drilling fluid (mud) is pumped down the drill string and up the annulus as in conventional drilling, but the mud is returned through a subsea pump and a separate return conduit. This differs from conventional drilling. The pump is used to control the level in the riser which in turn affects the pressure profile in the annulus. The objective is to maintain the pressure at each location in the well above the lower pore/collapse pressure and below the fracture pressure.

There are a few simplified models for DGD systems in the litterature. In Breyholtz and Nygaard (2009) and Breyholtz et al. (2011) an existing simplified model for MPD, presented in Kaasa et al. (2012), is modified to fit the DGD system. The model is used to implement a model predictive controller that coordinates control of the subsea pump and topside equipment. Hauge et al. (2012) present a simplified model of a gas bubble percolating up an open well-bore. The model can be used for control design and estimation during gas influx scenarios. We also mention the work by Landet (2011) where a high order model for MPD system is presented; the model is based on discretizing the partial differential equations describing a hydraulic transmission line. The author proposes a modification to the model so that multiple fluid scenarios can be simulated, but the reasoning behind the modification is not entirely clear.

The modelling effort in this paper builds on the model presented in Kaasa et al. (2012) and modified for DGD in Breyholtz et al. (2011). We model the pressure dynamics in the drill string based on a mass balance, taking compressibility into account. Since the annulus is open to the atmosphere (and thus not pressurized), we do not model compressibility effects of the drilling mud in the annulus, and consequently the mass balance results in a volume balance. The flow rate from the drill string to the annulus is modelled based on a momentum balance, as is the pressure at any location in the well/drill string. The key difference between the model derived here and the work in Breyholtz and Nygaard (2009) and Breyholtz et al. (2011) is that our model allows for two different types of fluids to be present in each section of the well (drill string, annulus, subsea pump and return lines); we also include a model of the centrifugal subsea pump. Besides the differences between a pressurized MPD system and a DGD system, our model differs from the one in Landet (2011) in that it has a lower number of control volumes and the underlying assumptions regarding the pressure dynamics are more transparent. Note that even though we constrain ourself to only two fluids in this paper, it is straight forward to extend the ideas to more than two fluids.

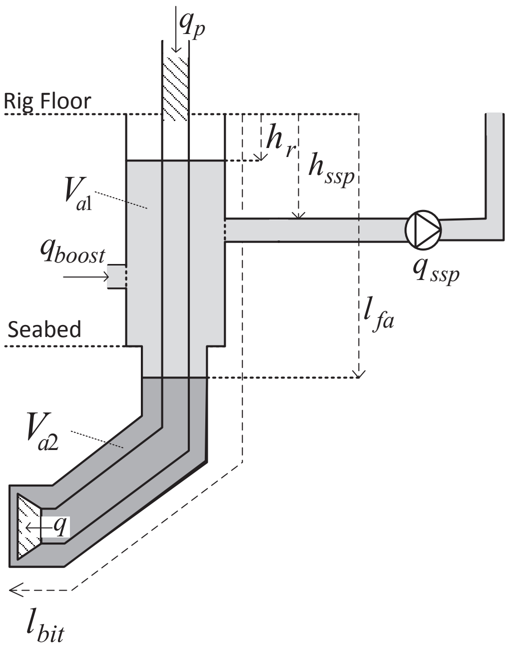

Fig. 1. Schematic of a dual gradient drilling system. Mud flows through the rig pump, down the drill string, through the bit, up the annulus and returns through a subsea pump. The level of mud in the riser, h_r, is increased or decreased to control the annular pressure.

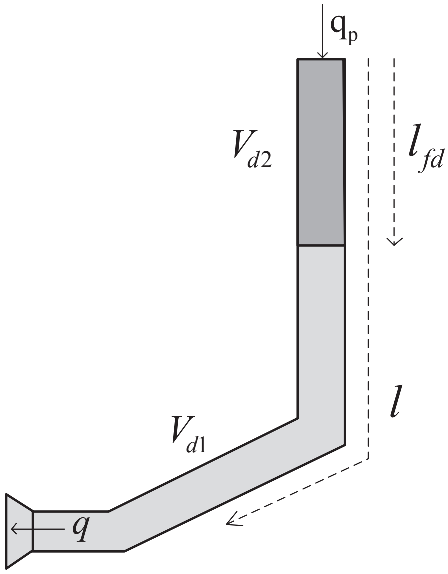

Fig. 2. The drill string contains two different fluids of volume V_{d1} and V_{d2}. As mud is pumped into the drill string the position of the front, l_{fd}, moves downward towards the bit.

2. MODELLING

2.1 Conservation of Mass

Drill string We model the drill string as a hydraulic system consisting of two fluids as shown in Fig. 2. Based on the conservation of mass and the isothermal equation of state we have

$$\frac{V_{d1}}{\beta_{d1}}\dot{p}_1 = -q - \dot{V}_{d1} \tag{1a}$$

$$\frac{V_{d2}}{\beta_{d2}}\dot{p}_2 = q_p - \dot{V}_{d2} \tag{1b}$$

where p denotes pressure, q denotes flow rate, V denotes volume and β denotes the isothermal bulk modulus (inverse of compressibility). The subscripts $d1$ and $d2$ refer to volumes 1 and 2 in the drill string. (1a) models the pressure variation at any location in V_{d1} while (1b) models the pressure variation at any location in V_{d2}.

Let p denote the pressure at any location in the drill string. We assume that the pressure change at any location in the drill string is the same, that is $\dot{p} = \dot{p}_1 = \dot{p}_2$. Adding the two equations together gives

$$\left(\frac{V_{d1}}{\beta_{d1}} + \frac{V_{d2}}{\beta_{d2}}\right)\dot{p} = -q - \dot{V}_{d1} + q_p - \dot{V}_{d2}. \tag{2}$$

Since the total drill string volume is (piecewise) constant we have that $\dot{V}_{d1} = -\dot{V}_{d2}$ which enables us to simplify (2) to

$$\left(\frac{V_{d1}}{\beta_{d1}} + \frac{V_{d2}}{\beta_{d2}}\right)\dot{p} = q_p - q. \tag{3}$$

The above equation approximates the pressure dynamics at any location in the drill string. One example is the pump pressure, p_p, just downstream the rig pump. The pump pressure dynamics is thus governed by

$$\left(\frac{V_{d1}}{\beta_{d1}} + \frac{V_{d2}}{\beta_{d2}}\right)\dot{p}_p = q_p - q. \tag{4}$$

Note that for $V_{d2} = 0$ this equation reduces to the drill string dynamic equation derived in Kaasa et al. (2012). When $V_{d1} > 0$ and $V_{d2} > 0$ the term $\frac{V_{d1}}{\beta_{d1}} + \frac{V_{d2}}{\beta_{d2}}$ shows that the combined compressibility of the fluids in the drill string affects the pressure dynamics.

To implement (4) it is neccessary to provide a relationship for calculating the volume of the different fluids. To that end we assume that the drill string is filled with fluid of Type 1 and Type 2 with initial volumes $V_{d1}(t_0)$ and $V_{d2}(t_0)$ respectively. Neglecting compressibility effects the volumes are given as the solution to

$$\dot{V}^c_{d1} = -q \tag{5}$$

$$\dot{V}^c_{d2} = q_p. \tag{6}$$

However, due to compressibility effects the above equations are not valid during transients. E.g. if the pressure is increased the above equations will overestimate the two volumes. To mitigate this problem we normalize the two volumes according to

$$V_{d1} = kV^c_{d1} \tag{7}$$

$$V_{d2} = kV^c_{d2} \tag{8}$$

where

$$k = \frac{V_d}{V^c_{d1} + V^c_{d2}}, \tag{9}$$

and V_d is the total internal volume of the drill string. This normalization ensures that $V_d = V_{d1} + V_{d2}$. Note that (7)–(9) does not take the different compressibilities of the fluids into account. That is, if fluid 1 is more compressible than Fluid 2, then Fluid 1 would compress relatively more than

Fluid 2. In the Appendix it is shown how to take this effect into account by using the definition of the bulk modulus. We will use the simple method as comparisons show that the approximation is quite good (less than one percent error) for the relevant choices of bulk moduli. The position of the front, l_{fd}, is simply given as the solution to

$$l_{fd} = \frac{V_{d2}}{A_d} \tag{10}$$

where A_d is the internal cross-sectional area of the drill string.

Annulus Similar to the derivation for the drill string we consider two different fluids of volume V_{a1} and V_{a2}, in the annulus as shown in Fig. 1. Since the annulus is open to the atmosphere we make the simplifying assumption that compressibility effects caused by pressure variations are negligible. The mass balance thus reduces to a volume balance. The flow through the bit and the flow from the booster pump both enter the annulus while the flow through the subsea pump exits the annulus. In this paper we make the simplifying assumption that $q_{boost} = 0$ which would typically be the case in multi-fluid scenarios. The total volume of fluid in the annulus, V_a, is governed by

$$\dot{V}_a = q - q_{ssp} \tag{11}$$

which implies that the riser level, h_r, satisfies

$$\dot{h}_r = \frac{q_{ssp} - q}{A_a(h_r)} \tag{12}$$

where $A_a(h_r)$ is the crossectional area of the annulus at location h_r. This equation is the same as the one used in Breyholtz et al. (2011) and Zhou and Nygaard (2011). For the the location of the front between the two fluid types we have two different scenarios. In scenario 1 Fluid 1 occupies the top part of the annulus includig the inlet to the subsea pump, while Fluid 2 occupies the bottom part of the annulus, as depicted in Fig. 1. In this case $l_{fa} \geq h_{ssp}$ and

$$\dot{l}_{fa} = \frac{-q}{A_a(l_{fa})} \tag{13}$$

In scenario 2 Fluid 2 occupies all of the well, except some small part above the suction hose going to the subsea pump. In this scenario

$$\dot{l}_{fa} = \dot{h}_r = \frac{q_{ssp} - q}{A_a(h_r)}. \tag{14}$$

Return lines The riser is connected to the subsea pump by a suction line, and the subsea pump is connected to the rig by a discharge line. The volumes in this part of the system is modelled similarly to the drill string giving

$$\dot{V}_{r1} = \begin{cases} 0 & l_{fa} > h_{ssp} \\ -q_{ssp} & l_{fa} \leq h_{ssp} \end{cases} \tag{15}$$

where V_{r1} is the volume of fluid 1 in the return lines. The volume of fluid 2 is $V_{r2} = V_r - V_{r1}$, where V_r is the total volume of fluid in the discharge line. The location of the fluid front, l_{fr}, is given by

$$l_{fr} = \frac{V_{r1}}{A_r}, \tag{16}$$

where A_r is the internal cross-sectional area of the return line.

Remark 1. Note that the model does not handle an oscillating riser level h_r that generates several disconnected volumes of Fluid 1 and 2 in the discharge line. If this is an issue the model can be extended by increasing the number of allowed fluid fronts in the return lines.

2.2 Momentum balance

To model the flow rate through the bit we use a momentum balance similar to the model in Kaasa et al. (2012) giving

$$M(h_r)\dot{q} = p_p - p_0 - F(l_{fd}, l_{fa}, h_r, q) + G(l_{fd}, l_{fa}, h_r) \tag{17}$$

$$M(h_r) = \int_0^{l_{bit}} \frac{\rho_d(l)}{A_d(l)} dl + \int_{h_r}^{l_{bit}} \frac{\rho_a(l)}{A_a(l)} dl \tag{18}$$

where p_0 is the atmospheric pressure, $F(l_{fd}, l_{fa}, h_r, q)$ is the total frictional pressure loss in the drill string and annulus, $G(l_{fd}, l_{fa}, h_r)$ describes the hydrostatic pressure difference between the drill string and the annulus, $\rho_d(l)$ and $\rho_a(l)$ are the densities, at location l, in the drill string and annulus respectively, l_{bit} is the length from the rig floor to the bit and finally $A_d(l)$ and $A_a(l)$ are the crossectional areas, at location l, in the drill string and annulus respectively. Note that F and G depend on additional parameters such as geometry and density. These arguments are omitted for notational convenience. More detailed expressions for these functions are given in (29) and (22).

In addition to the differential equation above we have that the pressure at any location in the well is given by a steady state momentum balance in the annulus according to

$$p_a(l) = p_0 + F_a(l, l_{fa}, h_r, q) + G_a(l, l_{fa}, h_r) \tag{19}$$

where $F_a(l, l_{fa}, h_r, q)$ is the frictional pressure drop, and $G_a(l, l_{fa}, h_r)$ is the hydrostatic pressure, from the top of the annulus to location l. A similar relationship can be formulated by applying a momentum balance in the drill string.

Hydrostatic Pressure Looking at Fig. 2 we see that the hydrostatic pressure at a location l in the drill string is given by

$$G_d(l, l_{fd}) = \begin{cases} \rho_{d2} g h(l) & l < l_{fd} \\ \rho_{d2} g h(l_{fd}) + \rho_{d1} g(h(l) - h(l_{fd})) & l \geq l_{fd} \end{cases} \tag{20}$$

where $h(l)$ is a function that returns the vertical depth at location l. Similarly for the annulus we have

$$G_a(l, l_{fa}, h_r) = \begin{cases} \rho_{a1} g(h(l) - h_r) & l < l_{fa} \\ \rho_{a1} g(h(l_{fa}) - h_r) + \rho_{a2} g(h(l) - h(l_{fa})) & l \geq l_{fa} \end{cases} \tag{21}$$

The total hydrostatic pressure difference used in (17) is given as

$$G(l_{fd}, l_{fa}, h_r) = G_d(l_{bit}, l_{fd}) - G_a(l_{bit}, l_{fa}, h_r). \tag{22}$$

For future reference the hydrostatic pressure in the return line, just upstream the subsea pump, is given as

$$G_r(l_{fr}) = \rho_{a1} g h(l_{fr}) + \rho_{a2} g(h_{ssp} - h(l_{fr})) \tag{23}$$

where l_{fr} is the fluid front in the return lines, found from (16).

Frictional Pressure Losses In general drilling fluids are non-Newtonian and the flow path will contain both laminar and turbulant flow regimes, and transitions between these regimes (Bourgoyne Jr. et al. (1991); Zamora et al. (2005); API (2006)). This makes detailed modelling of frictional losses a significant challenge. For high accuracy the so-called modified Herschel-Bulkley model is the industry choice. The modelling framework presented this far allows for any functional description of the pressure losses including non-Newtonian models. However, for clarity of presentation and brevity we will constrain ourself to Newtonian fluids from here on. For completness we state the main relationships and explain how we use them. A thorough account on viscous Newtonian flow is given in White (1994). First we consider Fluid 2 in the drill string. To determine if the flow regime is laminar or turbulent we use the Reynolds number

$$Re_{d2}(l) = \frac{4\rho_{d2}q}{\pi d_d(l)\mu_d} \tag{24}$$

where $d_d(l)$ is the drill string inner diameter and $\mu_d(l)$ the viscosity, at location l in the drill string. Given a location l and a flow rate q we can calculate the Reynolds number. If this number is below $Re_{crit} = 2300$ the flow is deemed to be laminar, if it is above then the flow is turbulent. To obtain the pressure loss we use the Darcy-Weisbach equation

$$F_{d2}(l_{fd}, q) = \int_0^{l_{fd}} f_{d2}(l)\frac{8\rho_d q^2}{\pi^2 d_d^5(l)}dl \tag{25}$$

where the friction factor is given by

$$f_{d2}(l) = \frac{64}{Re_{d2}(l)} \tag{26}$$

for laminar flow,

$$f_{d2}(l) = \left(-1.8log\left[\frac{6.9}{Re_{d2}(l)} + \left(\frac{\epsilon_d}{3.7d_d(l)}\right)^{1.11}\right]\right)^{-2} \tag{27}$$

for turbulent flow, and ϵ_d is the pipe wall roughness, see White (1994) and Haaland (1983). The pressure loss in the drill string consists of pressure losses in topside equipment, drill string (two fluids) and bottomhole assembly including the bit. For simplicity we consider only friction losses in the drill string and over the bit in this paper. The frictional pressure drop from rig pump to the bit is thus

$$F_d(l_{fd}, q) = F_{d2}(l_{fd}, q) + F_{d1}(l_{fd}, q) + \frac{\rho_d(l_{bit})q^2}{2C_v^2 TFA^2} \tag{28}$$

where $F_{d1}(l_{fd})$ is found from an expression similar to (25), C_v is the discharge coefficient and TFA is the total fluid area in the bit (API (2006)). The density at the bit, $\rho_d(l_{bit})$, is equal to ρ_{d1} as long as $l_{fd} < l_{bit}$, after that it is equal to ρ_{d2}. Similar derivations hold for the annulus friction pressure loss $F_a(l, l_{fa}, h_r, q)$, the suction line friction losses $F_{suc}(l_{fr}, q_{ssp})$ and the discharge line friction losses $F_{dis}(l_{fr}, q_{ssp})$. The total frictional pressure loss used in (17) is given by

$$F(l_{fd}, l_{fa}, h_r, q) = F_d(l_{fd}, q) + F_a(l_{bit}, l_{fa}, h_r, q). \tag{29}$$

2.3 Subsea Pump

The centrifugal subsea pump is used to pump fluid from the riser and up to the rig. The pump is typically controlled using a frequency converter which maintains the pump at a certain pump speed ω_{ssp}. In this paper we assume that the frequency converter ensures that ω_{ssp} converges to its reference ω_{ssp}^{ref} after a short transient period. That is, we model the actuator dynamics as

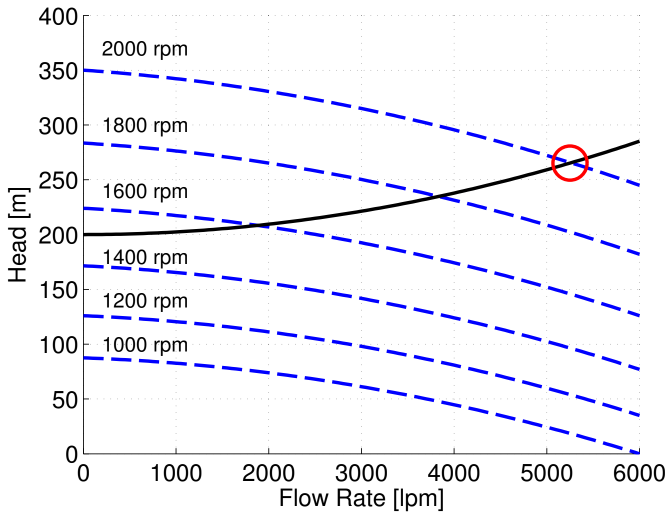

Fig. 3. Synthesised pump characteristics for subsea pump, top curve corresponds to $\omega_{ssp} = 2000$ rpm, bottom curve corresponds to $\omega_{ssp} = 1000$ rpm.

$$\tau_{ssp}\dot{\omega}_{ssp} = -\omega_{ssp} + \omega_{ssp}^{ref} \tag{30}$$

where τ_{ssp} is a time constant that models the frequency converter and rotor/impeller dynamics. Since the pump is dynamic (and not a positive displacement pump) the flow rate, q_{ssp}, depends not only on ω_{ssp}, but also on the total head. To take this effect into account we need to consider the pump curve/characteristic in the model. The pump characteristic is typically found through experimental testing and looks similar to the example shown in Fig. 3. The top dashed curve shows the total head that is produced by the pump at $\omega_{ssp} = 2000$ rpm, while the bottom dashed curve corresponds to $\omega_{ssp} = 1000$ rpm. As the flow rate increases the total head is reduced. The operational point of the pump is given by the intersection of the system curve (whole) with the pump curve. For $\omega_{ssp} = 2000$ this intersection is marked with a circle in Fig. 3. The system curve specifies the system head consisting of friction losses and hydrostatic head. Head is derived by dividing pressure by gravitational acceleration and the density of the fluid in the pump. If we reduce the pump speed to 1400 rpm corresponding to the third dashed curve from the bottom we see that the two curves do not intersect, this implies that the pump speed is not sufficient to pump the required hydrostatic head. Mathematically we can express these notions according to

$$h_{tot} = f_{ssp}(\omega_{ssp}, q_{ssp}) \tag{31}$$

where h_{tot} is the total head. Using the so called affinity laws (similartiy rules), see e.g. White (1994), it is not hard to approximate f_{ssp} from a limited set of experimental data. In this paper we assume f_{ssp} has the form

$$f_{ssp}(\omega_{ssp}, q_{ssp}) = c_0\omega_{ssp}^2 - c_1\omega_{ssp}q_{ssp} - c_2q_{ssp}^2 \tag{32}$$

where c_0, c_1, c_2 are fitting constants and ω_0 is the pump speed at which the curve was fitted. For the synthesised example in Fig. 3 we have $c_0 = 8.75 \times 10^{-5}$, $c_1 = 0.175$ and $c_2 = 7.00 \times 10^3$. Neglecting frictional effects in the riser the system curve is described by

	viscosity $[\frac{Ns}{m^2}]$	density $[\frac{kg}{m^3}]$	Bulk modulus [Pa]
Fluid 1	2×10^{-3}	1120	1.0×10^9
Fluid 2	4×10^{-3}	1200	1.5×10^9

Table 1. Drilling fluid properties.

$$h_{sys}(l_{fr}, q_{ssp}) = \frac{1}{g\rho_{ssp}} [G_r(l_{fr}) + F_{dis}(l_{fr}, q_{ssp}) \\ -(G_a(h_{ssp}, l_{fa}, h_r) - F_{suc}(l_{fr}, q_{ssp}))] \quad (33)$$

where ρ_{ssp} is the density of the fluid in the pump, the hydro static pressure components G_r and G_a are defined in (21) and (23), F_{dis} and F_{suc} the frictional pressure losses in the discharge and suction lines calculated as explained in the previous section. Given the rotational velocity of the pump, mud densities and the location of the different fluids, the operational point of the pump is given as the solution q^*_{ssp} to the implicit equation

$$h_{sys}(l_{fr}, q^*_{ssp}) = f_{ssp}(\omega_{ssp}, q^*_{ssp}). \quad (34)$$

A solution is guaranteed to exist only if ω_{ssp} is sufficiently high (e.g. over 1500 rpm in Fig. 3). When ω_{ssp} is not high enough $q_{ssp} < 0$, a scenario that we do not consider in this paper. That is, we assume that the solution q^*_{ssp} always exists.

3. SIMULATIONS

To illustrate the use of the model we also implement a standard PI controller according to

$$\omega^{ref}_{ssp} = -K_p \left(e(t) + \frac{1}{T_i} \int_0^t e(\tau) d\tau \right) \quad (35)$$

where K_p is the proportional gain, T_i is the integral time and the error is $e = p_a(l_{bit}) - p^{ref}_{bit}$ where $p_a(l_{bit})$ is the measured anulus pressure at the bit and p^{ref}_{bit} is the bit pressure reference. The controller is designed to maintain a constant bit pressure in a multi-fluid scenario. We chose the gains as $K_p = -0.0049$ and $T_i = 88s$ based on a step resonse test and the SIMC tuning rules in Skogestad and Postlethwaite (2007).

The simulation consists of a fluid change. To begin with the entire well is filled with fluid of Type 1, then fluid of Type 2 is pumped into the well displacing the original fluid. At the end of the simulation, the drill string, well, return lines and most of the riser are filled with fluid of Type 2. At the top of the riser there is some amount of Fluid 1 left. The parameters for the fluids are given in Table 1.

The well consists of a 300m long riser, a 1200m section with inner diameter 9.66" and a 2000m open hole section with inner diameter 8.5". The first 1500m of the well (including riser) are vertical followed by a 2000m horizontal section. Parameters for the simulation are given in Table 2. For simplicity we use the same wall roughness, ϵ_d in the entire well.

Fig. 5–7 shows results from the simulation. In the simulation $p^{ref}_{bit} = 175$ bar. At $t = 60$ min the fluid pumped through the rig pump is changed from Type 1 to Type 2. From Fig. 7 we can see that the fluid front in the drill string, l_{fd}, moves from zero to $l_{bit} = 3500$m over a period of about 20 minutes. During this period the pump pressure, p_p, first drops from 102 bar to 93 bar before increasing to 97 bar. This is caused by an increase

Param.	Description	Value
τ_{ssp}	Time constant, pump	3s
ϵ_d	Drill pipe roughness	2×10^{-3}mm
TFA	Total fluid area, bit	$5.01 \times 10^{-4} m^2$
C_v	Bit discharge coefficient	0.98
g	Gravitational acceleration	$9.81 \frac{m}{s^2}$
d_d	Inner diameter, drill string	0.1125m
d_{do}	Outer diameter, drill string	0.1270m
d_{ret}	Inner diameter, return line	0.152m
d_a	Inner diameter, wellbore	$[0.495, 0.245, 0.216]$m
l_{well}	Length coordinates	$[0, 300, 1500, 3500]$ m
h_{well}	Depth coordinates	$[0, 300, 1500, 1500]$m
l_{suc}	Length, riser to pump	50m
l_{dis}	Length, pump to rig floor	200m
h_{ssp}	Depth, rig floor to pump	200m
l_{bit}	Location of bit	3500m
p_0	Atmospheric pressure	1×10^5Pa

Table 2. Simulation parameters

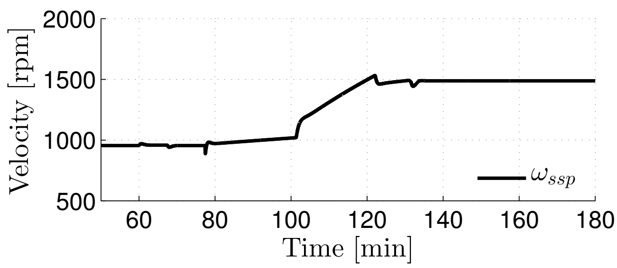

Fig. 4. Rotational velocity for the subsea pump.

in the hydrostatic pressure difference between the drill string and the annulus while the front is in the vertical section of the well, followed by increased friction as Fluid 2 moves along the horizontal section. Note that Fluid 2 has higher density and viscosity than Fluid 1. While Fluid 1 is displaced by Fluid 2 in the drill string there are only minor disturbances on the bit pressure which are compensated by minor adjustments to the pump speed, ω_{ssp}, by the PI controller.

At $t \approx 78$min the fluid front reaches the bit and starts to move up the annulus. We see that the front, l_{fa}, moves with a speed that is inversely proportional to the different annular cross-sectional areas, i.e. slows down as the area increases. In the beginning the level in the riser is lowered (h_r increases) slowly to compensate for increased friction, however when the front reaches the vertical section of the well the level in the riser falls (h_r increases) much faster to compensate for the heavier fluid displacing the lighter fluid.

When Fluid 2 reaches the riser (large diameter) the increase in h_r slows down. Finally, at $t \approx 130$min, Fluid 2 starts to displace Fluid 1 in the return lines creating a small disturbance at $t = 132$min ($l_{fr} = l_{ds} = 200$m) when Fluid 2 reaches the centrifugal pump.

4. CONCLUSIONS

We have extended existing work on simplified modelling of dual gradient drilling operations by allowing for multi-fluid operations. The model is suitable for control design, simulation and estimation. We only consider two different fluids in this paper but the ideas are readily extendable to more than two fluids. Although simulations show that the behaviour of the model is reasonable, the results presented

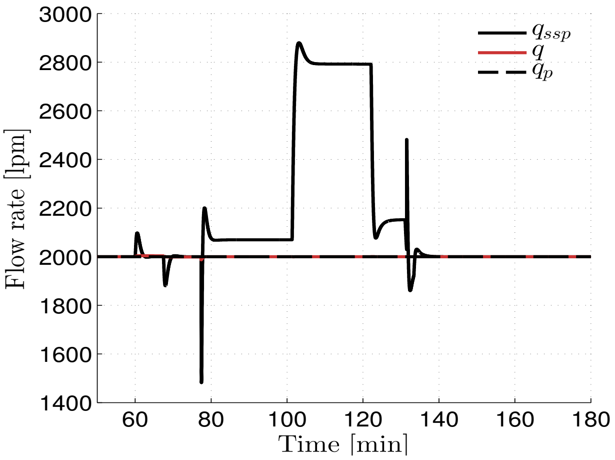

Fig. 5. Flow rates through rig pump, bit and subsea pump.

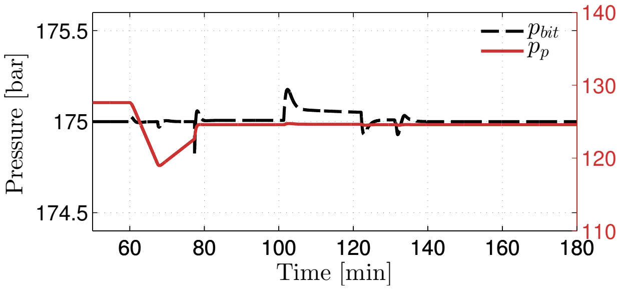

Fig. 6. Bit pressure (left axis) and pump pressure (right axis).

should be seen as preliminary until comparisons with high fidelity models and/or data can quantify the accuracy of the model. In addition future work should investigate the possibility of extending the model to allow for one of the fluids to be of gas phase.

REFERENCES

API (2006). Rheology and hydraulics of oil-well drilling fluids. *API Recommended Practice 13D.*

Bourgoyne Jr., A.T., Millheim, K.K., Chenevert, M.E., and Young Jr., F.S. (1991). *Applied Drilling Engineering.* Society of Petroleum Engineers.

Breyholtz, Ø. and Nygaard, G. (2009). Evaluating new and existing automatically controlled deep water drilling concepts using a high-fidelity simulation model. In *Proc. Scandinavian Conf. on Simulation and Modeling.*

Breyholtz, Ø., Nygaard, G., and Nikolaou, M. (2011). Managed pressure drilling: Using model predictive control to improve pressure control during dual-gradient drilling. *SPE D&C*, 26, 182–197.

Fossli, B. and Sangesland, S. (2006). Controlled mud-cap drilling for subsea applications: Well-control challenges in deep waters. *SPE Drilling & Completion*, 21, 133–140.

Haaland, S.E. (1983). Simple and explicit formulas for the friction factor in turbulent pipe flow. *Journal of Fluids Engineering*, 89–90.

Hauge, E., Godhavn, J.M., Stamnes, Ø.N., and Aamo, O.M. (2012). A dynamic model of percolating gas in an open well-bore. *7th Vienna Int. Conf. on Mathematical Modelling.*

Kaasa, G.O., Stamnes, Ø.N., Imsland, L., and Aamo, O.M. (2012). Simplified hydraulic model used for intelligent estimation of downhole pressure for an MPD control system. *SPE Drilling & Completion*, 27(1), 127–138.

Landet, I.S. (2011). *Modeling and Control for Managed Pressure Drilling from Floaters.* Master's thesis, Norwegian University of Science and Technology.

Schumacher, J.P., Dowell, J.D., Ribbeck, L.R., and Eggemeyer, J.C. (2002). Planning and preparing for the first subsea field test of a full-scale dual-gradient drilling system. *SPE Drilling & Completion*, 17, 194–199.

Skogestad, S. and Postlethwaite, I. (2007). *Multivariable Feedback Control.* John Wiley & Sons, Ltd.

White, F. (1994). *Fluid Mechanics.* McGraw-Hill.

Zamora, M., Roy, S., and Slater, K. (2005). Comparing a basic set of drilling fluid pressure-loss relationships to flow-loop and field data. In *Proc. AADE National Technical Conf. and Exhibition.*

Zhou, J. and Nygaard, G. (2011). Automatic model-based control scheme for stabilizing pressure during dual-gradient drilling. *Journal of Process Control*, 21(8), 1138–1147.

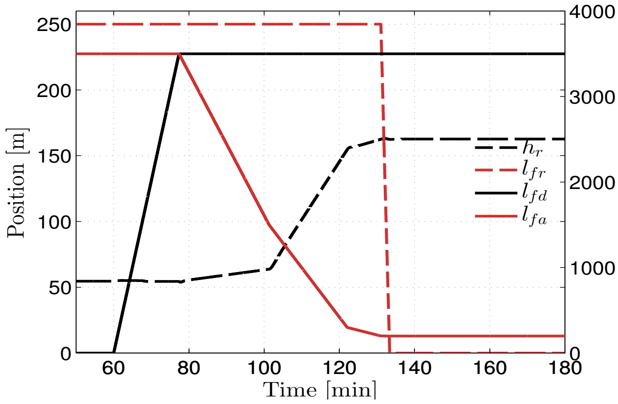

Fig. 7. Riser level, location of fluid fronts in the drill string, annulus and return line. Dashed lines belong to left axis and whole belong to right axis.

Appendix A

To more accurately normalize the volume calculations from Section 2.1 one can take the different compressibilities into account. To take this effect into account we use the bulk modulus, which for Fluid 1 is defined as

$$\beta_{d1} = -V_{d1}^c \frac{\Delta p}{(V_{d1} - V_{d1}^c)} \tag{A.1}$$

That is, for a given pressure difference Δp the volume is compressed from V_{d1}^c to V_{d1}, where V_{d1}^c is the solution to (5). Rearranging we get

$$V_{d1} = V_{d1}^c \left(1 - \frac{\Delta p}{\beta_{d1}}\right) \tag{A.2}$$

Similarly for fluid 2 we have

$$V_{d2} = V_{d2}^c \left(1 - \frac{\Delta p}{\beta_{d2}}\right) \tag{A.3}$$

where V_{d2}^c is the solution to (6). In the above equations we have three unknowns V_{d1}, V_{d2} and Δp and it is therefore necessary to add an additional relationship. For this purpose we use the knowledge that the known drill string volume, V_d, satisfies

$$V_d = V_{d1} + V_{d2} \tag{A.4}$$

We now have three independent equations so we can solve for the three unknowns.